Malaysian Journal of Chemistry, 2023, Vol. 25(3), 74-86
(Special Issue: *2nd Applied Science Research International Conference 2022*)

Electrocoagulation with Vibration-induced Electrodes: Assessment of Plate Resistance and Flocculation Behaviour

Noorzalila Muhammad Niza[1*] and Mohamad Anuar Kamaruddin[2]
[1]Chemical Engineering Studies, College of Engineering, Universiti Teknologi MARA Penang Branch, 13500 Permatang Pauh, Pulau Pinang, Malaysia
[2]Environmental Technology Division, School of Industrial Technology, Universiti Sains Malaysia, 11800, Gelugor, Pulau Pinang, Malaysia
*****Corresponding author (e-mail: zalila2871@uitm.edu.my)

The role of gas bubbles in electrocoagulation is significant as it will determine the efficient mass transfer of the coagulant ions and help in the flocculation-flotation process. However, the drawbacks on the accumulation and adherence of gas bubbles on the electrode surface during the treatment have not been thoroughly studied and the particles distribution behaviour have not been the main focused in research on the enhancement and modification made on the electrocoagulation. This study assessed the plate resistance, zeta potential, kinetics of coagulation-flocculation and particle distribution behaviour of a new batch-electrocoagulation treatment with vibration-induced electrodes. It was determined that treatment using the electrocoagulation with vibration-induced plate showed 4 – 20% reduction on the plate resistance compared to electrocoagulation with stationary plates. In addition, the electrocoagulation with vibration-induced plates approached a faster rate of coagulation-flocculation with the Brownian diffusion kinetic data followed the second order reaction and a rate constant of 0.0001 $L.mg^{-1}min^{-1}$. From the particle distribution behaviour, the coagulation-flocculation mechanism of the electrocoagulation was dominantly achieved through charge neutralization. The vibration of electrodes able to improve the performance of electrocoagulation by reducing the bubbles adherence and accumulation surrounding the electrode plates leading to enhanced plate resistance compared to stationary plates.

Keywords: Coagulation-flocculation kinetic; electrocoagulation; particles distribution behaviour; plate resistance; vibration-induced electrodes

Received: August 2022; Accepted: January 2023

Electrocoagulation can be defined as the destabilization of a colloidal suspension or solution through dissolution of anode electrode, where the destabilized particles are propagated to gather and agglomerate into larger flocs, and then removed by flotation [1, 2]. This technique is different from the coagulation-flocculation method as the electric current is applied to the connecting aluminium (Al) or iron (Fe) electrodes which are immersed in the wastewater. Theoretically, the release of cations during the electrocoagulation process is expected to reduce the repulsive energy (energy barrier) between the particles. With less repulsive forces between them, the particles can then be destabilized to form agglomerates that allow for easier separation of the sludge from the treated water [2].

In electrocoagulation, mixing is necessary to help coagulant to disturb stability in the colloidal system. The opportunity for the destabilized particles to collide requires some form of fluid motion, which can be achieved either by mechanical stirring or flow, or both. Most of the previous studies that used electro-coagulation were based on the conventional reactor composed of static electrode plates and magnetic stirrer or overhand stirrer to agitate the solution [3–5]. Without any agitation mechanism, the biggest disadvantage of utilizing static electrode in batch electrocoagulation is that it produces almost stagnant flow in the reactor which require a long reaction time for an efficient treatment of metal ions and salt removal [6]. Inefficient solution mixing also reduces mass transfer during the process because of poor molecular diffusion, leading to the formation of a passive film on the electrode surface which then increased the resistance and energy consumption of the process [7].

Electrocoagulation can be categorized as a gas-evolving system because the hydrogen and oxygen are produced in parallel with the coagulants generation at the anode. These gases produce bubbles on the surface of the electrodes, dispersed to the bulk solution which then help in the flocculation (attachment with the colloid particles which produce sludge) and subsequently the sludge is separated to the top by flotation. With static electrodes or at low current density, gas bubbles provide self-circulation in the solution which promote directional growth, causing flow mix and fresh solution incoming without extra power required [8]. However, the self-

†Paper presented at the 2nd Applied Science Research International Conference 2022 (2nd ASRIC 2022)

circulation only produces slow mix which not able to avoid the ohmic overpotential caused by the undesired blockage by gas bubbles surrounding the electrode plates.

The ohmic potential arises from the resistance to flow of current between the electrodes. This resistance contains both an ionic component from the flow of charge chemical species through the electrolyte and an electronic component from the flow if electrons through the external [9]. The ohmic overpotential dynamically evolves as bubbles nucleate, grow and detach form the electrode surface which periodically affect the overall resistance of the electrolyte. The oxygen (O_2) and hydrogen (H_2) gas bubbles that are generated during the process will accumulate at the surface of the electrodes and increase the electrical resistance between the electrodes, thereby resulting in a less than optimum ionic transfer. As such, an uneven formation of gas bubbles on the electrode surface can lead to a concentration of gas bubbles in the specific zone of flotation. Consequently, a high electrolytic flow is required to minimize accumulation and detach bubbles from the surface of the electrode plates.

Several techniques are available for the removal of accumulated bubbles which can be grouped into passive or active methods. In the passive method, no additional energy source is needed to promote a change in bubble-evolution behavior while in the active method some external source for actuation is employed [9]. Example of passive methods can be either by geometrical approach, control on the nucleation bubble site or improve the electrolyte formulation. In a previous study on the control of nucleation bubble site, a novel design of a ring microelectrode encircling a hydrophobic micro-cavity under alkaline water electrolysis condition was effective in avoiding bubble coverage [10]. The chrono-potentiometric fluctuations of the cell were found to be weaker than in conventional microelectrodes. Numerical transport modeling helped to explain how bubbles forming at the cavity reduce concentration overpotential by lowering the surrounding concentration of dissolved gas. However, it was found that this design can aggravate the ohmic overpotential by blocking ion- conduction pathways.

On the other hand, the active methods make use of external forces to prevent bubble nucleation or induce early attachment, mitigating the impact of bubbles in the overpotential of the system [9]. Examples of this technique include use of shear flow, magnetic and acoustic field. Introducing shear flow in electro-coagulation by using magnetic stirrer bar or any other type of mechanical force is the example of flow technique. Effective shear flow rate over bubbles can induce early detachment and smaller detachment radii. It has been demonstrated that nucleation rate and the volume of detaching bubbles show a non-linear dependence on the shear rate, in particular, high flow rates lead to detachment of smaller bubbles and generate improved particle collision rate during flocculation [11, 12]. It was also observed that with increased applied voltage, the bubbles detach at smaller radii, attributed to the influence of convection induced by detaching bubbles and electrostatic repulsions between the bubbles and the electrodes.

Previous study on the application of electro-coagulation with vibration-induced electrode plates showed good performance in reducing the colour, COD and ammoniacal nitrogen in landfill leachate (Muhammad Niza et al., 2021; Muhammad Niza et al., 2020). Without requiring any external force to supply gas bubbles, vibrations were applied to the electrode plates using motor vibrators to help intensity in-situ microbubble generation. The gas bubble's action helped enhance the parallel flotation-flocculation process in electrocoagulation (Muhammad Niza et al., 2020). In this study, to further determine the performance difference, the assessment of plate resistance, zeta potential, coagulation-flocculation kinetics and particle distribution behaviour on electrocoagulation with vibrating electrodes were investigated. Results obtained from electrocoagulation with stationary plates were used for comparison in terms of the performance.

EXPERIMENTAL

Leachate Sampling and Preservation

The raw materials used for the electrocoagulation was the landfill leachate sampled at the retention pond at Pulau Burung Sanitary Landfill, Southern Penang, Malaysia (geographic coordinates of 5° 12′ N Latitude, 100° 25′ E Longitude). The samples were collected into 20 L clean PTFE carboys, which were completely filled with leachate to leave no space for aeration. The samples were collected via grab sampling within the consistent sampling points at the retention pond. Prior to further analysis in the laboratory, the samples were stored and preserved at 4 °C to avoid change in samples. The Standard Method for the Examination of Water and Wastewater [16] was referred for all the sampling, collection, storage and preservation methods.

Effect of Plate Resistance on Electrocoagulation

Figure 1 shows the electrocoagulation reactor used for the investigation of plate resistance. The electro-coagulation reactor with the working volume of 2 L consists of a pair of aluminium electrode plates (200 mm (L) x 50 mm (W), 1 mm thickness), each attached with a motor vibrator to induce vibration during the treatment. The aluminium plates have a total active surface area of 120 cm^2 immersed in the solution. Both electrode plates as well as the motor vibrators were connected with a digital DC power supply (of model QJE PS3005, China) which has the capability to supply between 0-10 A and 0-30 V of power. The determination of plate resistance during the electro-coagulation treatment of leachate for both vibration-

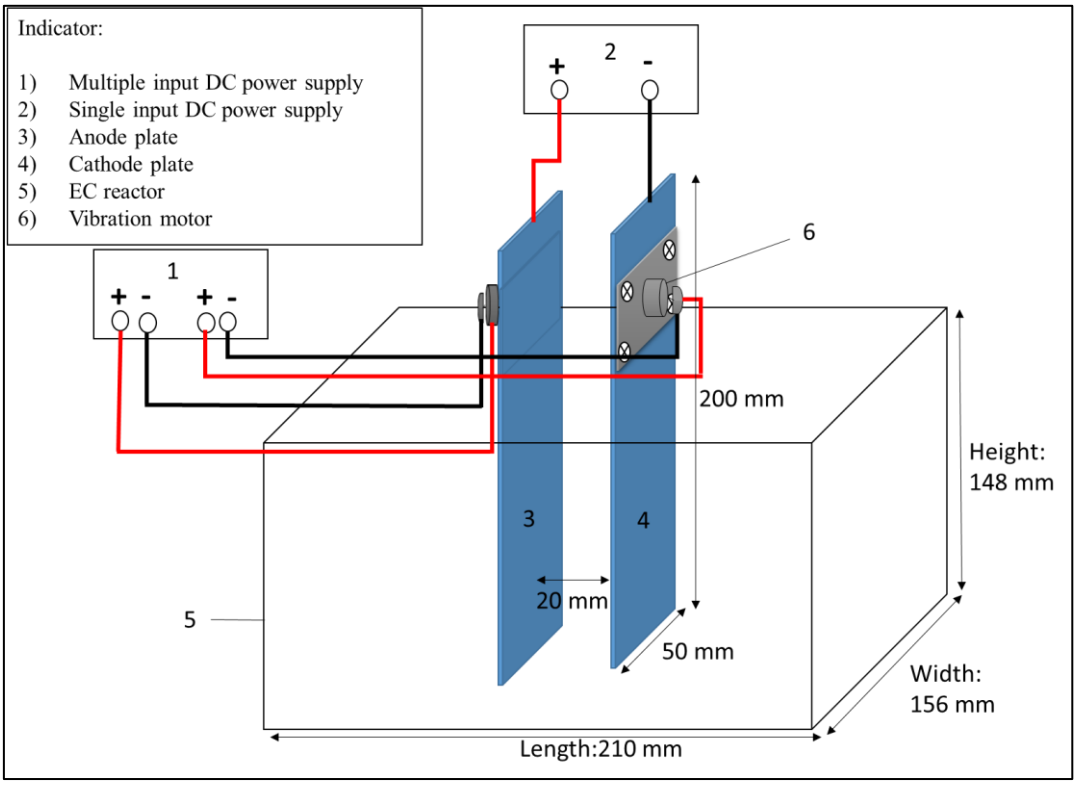

Figure 1. Schematic diagram of the batch electrocoagulation with vibration-induced electrode plates

induced and stationary electrode plates were made at a constant initial pH of 5 and at time intervals of 10 minutes (total treatment time of 60 minutes) with varied current intensities from 0.5 to 4.5 A and at constant vibration intensity of 2.8 V (the optimum vibration intensity as obtained in (Muhammad Niza et al., 2020). During the treatment, the electrode plates distance was fixed to 2 cm gap throughout the treatment.

The distance between electrodes can be related to the internal resistance measured by the Ohmic or IR drop, which is referred to the difference in potential required to transfer the ions through the solution. The internal resistance (R_m) can be calculated by the following equations [17]:

$$R_m = \frac{ID}{Ak} \quad (1)$$

where R_m is referred to the internal resistance of the medium between electrodes (medium), I is the electric current (A), D is the distance between the electrode (m), A is the active surface area of the anode (m^2) and k is the specific conductivity (mS/m). The resistance is also related with the Ohm's law as shown in Equation 2, where V is the voltage (volt) of the system and R_T is the total resistance of the medium, R_m and the plate resistance, R_p as shown in Equation 3. From these equations, it can be seen that as the electrode distance increases, this would indirectly increase the IR drop or the resistance of the solution. For this reason, the applied voltage should be increased to keep a constant current input to the system.

$$V = IR_T \quad (2)$$

$$R_T = R_m + R_p \quad (3)$$

Zeta Potential Analysis for Colloidal Stability

The zeta potential analysis was performed to determine the colloidal stability performance between vibration-induced and stationary electrode plates. The stability of leachate was analyzed by means of a Zetasizer Nano Series (Malvern Instrument, UK). Measurement for zeta potential analysis were taken for raw leachate samples and treated leachate samples with adjusted pH. The electrocoagulation with both vibration-induced and stationary electrode plates were subjected to 60 minutes of treatment at initial pH 5, current intensity of 3.5 A and vibration intensity of 2.8 V. Along the experimental run about 5 ml of sample was taken at 10, 23, 35, 48 and 60 minutes following the operating time used in this study. About 1 ml of sample was transferred into disposable folded capillary cuvette (DTS1070, Malvern, UK) and the zeta potential measurement was performed at temperature of 25 °C with distilled water as the dispersal medium.

Table 1. Degree of colloid stability as a function of zeta potential (Wang. et al., 2005).

Colloid stability	Zeta potential (mV)
Rapid coagulation or flocculation	from 0 to ±5
Incipient stability	from ±10 to ±30
Moderate stability	from ±30 to ±40
Good stability	from ±40 to ±60
Excellent stability	more than ±61

Table 2. Degree of coagulation as a function of zeta potential (Shammas, 2005).

Degree of coagulation	Zeta potential (mV)
Maximum	+3 to 0
Excellent	-1 to -4
Fair	-5 to -10
Poor	-11 to -20
Virtually none	-21 to -30

Table 1 and Table 2 were referred to assess the degree of colloidal stability and degree of coagulation as a function of zeta potential, respectively (Wang. et al., 2005; Shammas, 2005). The magnitude of the zeta potential is determined from electrophoretic measurement of particle mobility in an electric field (Wang. et al., 2005). From Table 1 and 2, it can be summarized that the lower the value of the zeta potential, the lower is the magnitude of the repulsive power between the particles, hence the less stable is the colloidal system. At this state of destabilization, effective coagulations can be achieved which would allow the particles to coming together and to form agglomerates. When zeta potential approaches 0 mV, the optimum destabilization would occur [2].

Coagulation-flocculation Kinetics using Brownian Diffusion

Colloids exhibit Brownian diffusion (*perikinetic* agglomeration), fluid motion (*orthokinetic* agglomeration) and differential sedimentation. Particle's thermal energy causes particles to have random motion in water; this motion is called Brownian motion and causes *perikinetic* aggregation [20]. The Brownian movement comprises colloids exhibiting a continuous random movement caused due to bombardment by water molecules in the dispersion medium [21]. This movement imparts kinetic energy to the particles causing an increase in the collision frequency and promoting coagulation and flocculation. Hence, the kinetics of electrocoagulation controlled by the Brownian diffusion was investigated for colour removal in leachate. The kinetic models were studied at optimum vibration intensity of 2.8 V vibration-induced plates, with the current intensity was varied accordingly from 0.5 – 4.5 A, constant initial pH of 5, and the sample volume of 2 L and initial temperature were kept constant. The total testing time was 60 minutes and the samples were taken at 10-minute intervals.

For Brownian coagulation of monodispersed particles at the early coagulation and flocculation stages, the rate of successful collision between particle sizes is described by the following equation modelled by Von Smoluchowski (1917) and Menkiti et al. (2011):

$$\frac{dC_n}{dt} = \frac{1}{2}\sum_{i+j=n} k_{ij} C_i C_j - C_N \sum_{i=1}^{\infty} k_{in} C_i \ldots\ldots\ldots (4)$$

where k_{ij} is the rate constant that controls the coagulation rate between an i-fold and j-fold cluster, t is the time, and $C_{n(t)}$ is the time-dependent number concentration of n-fold clusters. The authors further described the early Brownian kinetic coagulation of individual scattered particles by the rate expressed in Equation 5 [24]:

$$-r_p = -\frac{dC}{dt} = kC_t^{\alpha} \quad (5)$$

where $-r_p$ is the rate of decrease in the concentration of particles, C_t is the total particle concentration at time t, k is the rate constant, α is the reaction order of coagulation.

The experimental data for both electro-coagulation with vibration-induced and stationary electrode plates was fitted into the linearized form and was inspected the line of best-fitting when $\alpha = 1$ (first - order reaction) and $\alpha = 2$ (second - order reaction). For the first order reaction, integration of Equation 5 gives the following equation:

$$\ln [C]_t = -k_1 t + ln[C]_0 \quad (6)$$

where C_t and C_0 denote the colour concentration at time t and initial concentration in mg/L, respectively, and first-order rate constant k_1 in min^{-1}. Similarly, the linearized form of the second-order reaction can be described by Equation 7:

$$\frac{1}{C_t} = k_2 t + \frac{1}{C_0} \quad (7)$$

where k_2 is the second-order rate constant in L/mg.min.

A linear trend of the plot for Equations 6 and 7 indicates the reaction rate constant, i.e., the slope of the trend line indicates the rate constant *k*, based on each integrated rate law equation given for each reaction order. The best-fit kinetic model representing electrocoagulation with vibration-induced and stationary plates was selected based on the squared correlation coefficient, R^2.

Particle Distribution Behaviour Analysis

The particle distribution behaviour of the coagulation process can be presented graphically as concentration versus time. The particle distribution is denoted by C_i, where C is the concentration and subscripts i indicate monomer, doublet, and triplet for 1, 2, and 3, respectively. The particle distribution plots principally show the pattern and distribution of ion/particle aggregation as they flow into the visible droplet.

For Brownian aggregation, a generic expression for the time evolution of particles of the n-th order can solve the Von Smoluchowski equation for collision opportunities. The general form of the particle of the n-th order is shown by Equation 8 (Menkiti et al., 2011; Menkiti & Ejimofor, 2016; Ugonabo et al., 2012; Ugonabo et al., 2016):

$$\frac{C_n(t)}{C_0} = \frac{\left[\frac{t}{\tau_{R1/2}}\right]^{n-1}}{\left[1+\frac{t}{\tau_{R1/2}}\right]^{n+1}} \quad (8)$$

Hence, the time evolution for singlets (C_1), doublets (C_2) and triplets (C_3) can be solved by Equation 9-11: For monomer particles (singlets), when n = 1, Equation 8 yields:

$$C_1 = C_0\left[\frac{1}{\left[1+\frac{t}{\tau_{R1/2}}\right]^2}\right] \quad (9)$$

For doublets (dimers), when n = 2, Equation 8 yields:

$$C_2 = C_0\left[\frac{\frac{t}{\tau_{R1/2}}}{\left[1+\frac{t}{\tau_{R1/2}}\right]^3}\right] \quad (10)$$

For triplets (trimers), when n = 3, Equation 11 holds.

$$C_3 = C_0\left[\frac{\left[\frac{t}{\tau_{R1/2}}\right]^2}{\left[1+\frac{t}{\tau_{R1/2}}\right]^4}\right] \quad (11)$$

The rapid coagulation time (τ_R) and rapid coagulation half-life ($\tau_{R1/2}$) can be estimated using the following equations:

$$\tau_R = \frac{1}{C_0 k} \quad .(12)$$

$$\tau_{R1/2} = \frac{1}{0.5 C_0 k} \quad (13)$$

RESULTS AND DISCUSSION

Effect of Plate Resistance on Electrocoagulation

The total resistance (R_T) encountered during electro-coagulation is the summation of plate resistance (R_p) and internal resistance in the solution (R_m). Table 3 shows the R_T which was calculated using Equation 2 and R_m which was calculated using Equation 1. It can be seen from Table 3 that the resistance during the electrocoagulation was dominantly governed by the R_p since the value of R_p is higher than the R_m.

As seen in Equation 1, the R_m was proportionally dependent on the electrical current and distance of the electrode. Therefore, when the distance and effective surface area of the electrode remained constant during the stationary and vibrated-plate experiments, the R_m increased as the current intensity increased from 0.5 A

Table 3. The calculated resistance of electrocoagulation.

Current Intensity (A)	Total resistance, R_T (ohm)		Internal Resistance, R_m (ohm)	Plate Resistance, R_p (ohm)	
	Stationary plate	Vibration-induced plate		Stationary plate	Vibration-induced plate
0.5	4.11	3.77	0.0030	4.11	3.77
1.5	3.07	2.79	0.0090	3.06	2.78
2.5	2.75	2.21	0.0150	2.74	2.19
3.5	2.44	2.34	0.0212	2.42	2.32
4.5	2.24	2.14	0.0273	2.21	2.11

to 4.5 A. Nevertheless, the R_m of the solution was not as significant as the R_p. As seen in the same Table 3, the values of R_p and R_T was higher than the R_m for both in electrocoagulation with vibration-induced and stationary plates. The R_T and R_p was found to reduce when the current intensity increased from 0.5 A to 4.5 A. The resistance increased at low current intensity due to the accumulation of gas bubbles surrounding the electrode plates. The amount of bubbles on the surface of an electrode will increase as the current intensity increases [28]. This is true since by observation it can be seen that at the highest current intensity of 4.5, the plate and total resistance were found to be the lowest. An increase in current intensity to 4.5 A could also lead to greater upward momentum flux that carries pollutants to the top of the solution where it will cluster for easy collection and removal. A similar phenomenon is expected if the current intensity is increased to more than 4.5 A. Conversely, while low-current intensities at 0.5 A will produce relatively fewer bubbles, it results in lesser upward momentum flux and only a gentle agitation [29]. Therefore, low currents facilitate the accumulation and adherence of gas bubbles that raise the R_p, thereby, preventing the effective transfer of ions between plates.

In comparing the R_p between the electro-coagulation with vibration-induced and stationary plates as depicted in Figure 2, it was determined that when utilizing the vibration-induced plates the R_p was found to be 4% - 20% lower than the one obtained by stationary plates. The reduction in R_p when vibration-induced electrode plates were utilised indicated possible gas bubbles detachment as well as low bubble accumulation and adherence to the plates during vibration (Muhammad Niza , et al., 2020).

Flocculation Behaviour in Electrocoagulation with Vibration-induced Electrode Plates

Zeta Potential Analysis

Zeta potential can be used to further illustrate the efficient mechanism of pollutant removal using vibration-induced electrocoagulation in comparison to stationary plates. The zeta potential of raw leachate with no pH adjustment was -15.9 mV. The colloidal particles of the raw leachate were in incipient stability phase and coagulation activity was poor according to Tables 1 and 2 for the degree of stability and degree of coagulation, respectively. Figure 3 depicts the zeta potential of electrocoagulation at initial pH of 5 as a function of time. During electrocoagulation, the magnitude of the zeta potential when using both stationary and vibration-induced plates reduced. Based on the degree of stability and degree of coagulation, this low magnitude indicated that the repulsive forces between the particles reduced, thereby, allowing the electrostatic forces between the particles to increase and form agglomerations. At this stage, the solution rapidly flocculates resulting in better pollutant removal efficiency.

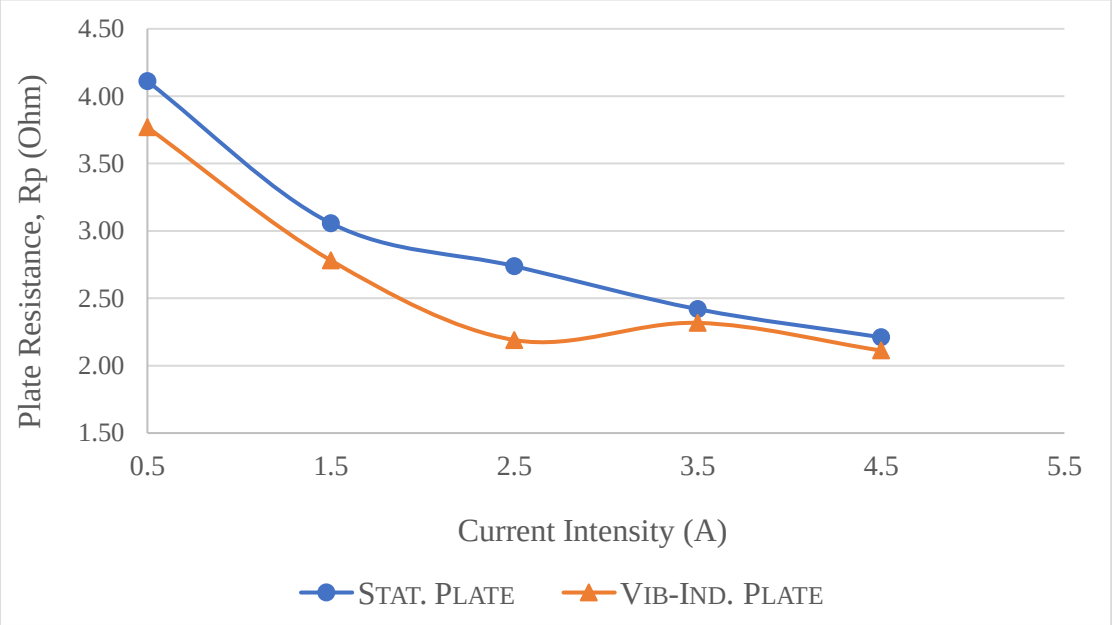

Figure 2. Effect of current intensity on plate resistance (R_p) in stationary vs. vibration-induced electrode plates

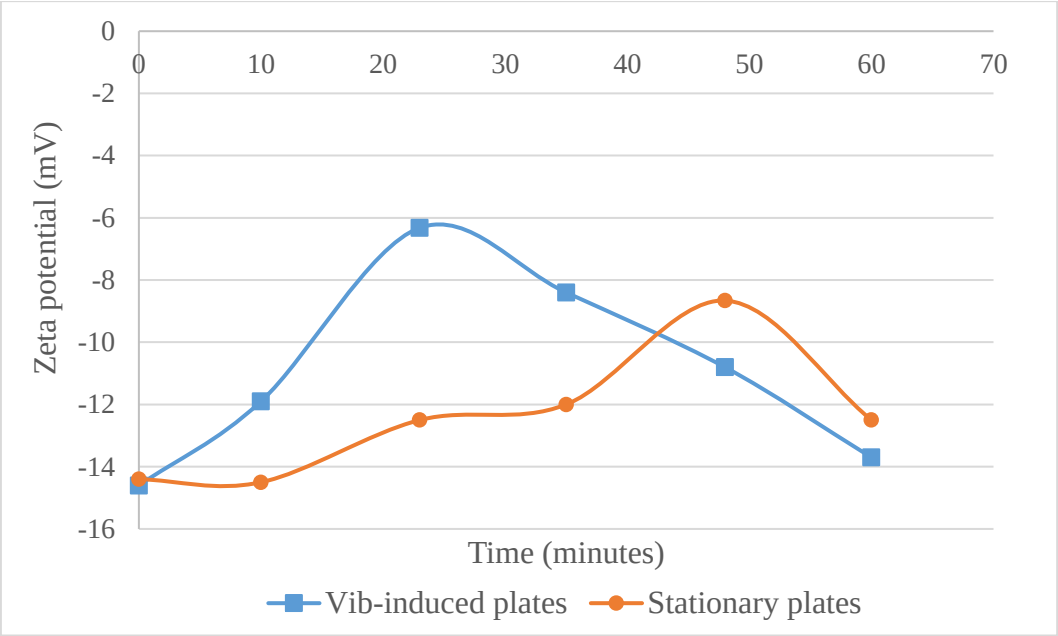

Figure 3. Effect of zeta potential on electrocoagulation using stationary vs. vibration-induced plates

In comparison to stationary plates, the synergistic effect of utilising vibration-induced plates in electrocoagulation is evident from the rapid coagulation-flocculation mechanism. As seen in the plots, the zeta potential of electrocoagulation using vibration-induced plates approached rapid coagulation or flocculation at approximately -6 mV within 20 to 30 minutes while it required 50 minutes to approach maximum coagulation-flocculation when using stationary plates. Although both stationary and vibration-induced plates only produced a fair degree of coagulation, the intensification of gas bubble action by the vibration-induced plates contributed to better pollutant removal efficiency, as explained by the faster rate of coagulation-flocculation through zeta potential. After it achieved the rapid coagulation or flocculation, both plots showed a reduced in the value of the zeta potential after optimum time, indicating that the flocculation occurred during this period.

The faster rate of coagulation-flocculation in electrocoagulation with vibration-induced plates can be explained by the efficient mixing which distributed coagulants and generated rapid collisions of bubbles-particles to form agglomeration or flocs. In electrocoagulation using stationary plates, a natural mixing force was created by the circulation of bubbles produced on the electrode surface. Nevertheless, the mixing was not intense thus requires a longer period of time for the destabilisation of particles.

Coagulation-flocculation Kinetic Study

The kinetics of electrocoagulation with vibration-induced and stationary plates were studied to investigate whether kinetics parameters and data follow the Brownian diffusion theory of coagulation-flocculation suggested by Von Smoluchowski [1917]. Electrocoagulation kinetics for vibration-induced and stationary plates at each current density are provided in Tables 4 and 5, respectively. The reaction rate constants, k_1 and k_2, and the regression coefficients (R^2) were determined for first- and second-order models. Reaction order plots are depicted in Figures 4 and 5. The curve is a better fit as R^2 approaches 1 [30]; this was used as the criterion to monitor whether electrocoagulation aligns with Brownian diffusion kinetics.

Table 4. Kinetic rate constants and R^2 in batch electrocoagulation with vibration-induced plates

Current density (mA/cm²)	**First order** $r_p = -\frac{dC}{dt} = k_1 C$		**Second order** $r_p = -\frac{dC}{dt} = k_2 C^2$	
	k_1 **(min⁻¹)**	R^2	k_2 **(L.mg⁻¹min⁻¹)**	R^2
4.2	0.0117	0.9448	4 x 10^{-6}	0.9405
12.5	0.0477	0.9668	6 x 10^{-5}	0.9577
20.8	0.0516	0.9067	8 x 10^{-5}	0.9535
29.2	0.0552	0.8935	9 x 10^{-5}	0.9814
37.5	0.0556	0.8540	0.0001	0.9890

Table 5. Kinetic rate constants and R^2 in batch electrocoagulation with stationary plates

Current density (mA/cm^2)	First order $r_p = -\frac{dC}{dt} = k_1 C$		Second order $r_p = -\frac{dC}{dt} = k_2 C^2$	
	k_1 (min^{-1})	R^2	k_2 ($L.mg^{-1}min^{-1}$)	R^2
4.2	0.0087	0.866	3×10^{-6}	0.8392
12.5	0.0496	0.9812	6×10^{-5}	0.9084
20.8	0.0541	0.9615	8×10^{-5}	0.9502
29.2	0.0551	0.9445	9×10^{-5}	0.9541
37.5	0.0530	0.9352	8×10^{-5}	0.9174

As seen in Tables 4 and 5, electrocoagulation R^2 values for vibration-induced plates showed that the process data best fits with the theory of flocculation as proposed by Von Smoluchowski (1917), where it is considered a second-order reaction, corresponding to R^2 of 0.9890 at 37.5 mA/cm^2, and 0.0001 $L.mg^{-1}min^{-1}$ reaction rate constant. Meanwhile, the first-order reaction best fits with electrocoagulation with stationary plates at a reaction rate constant of 0.0496 min^{-1}. The rate constant k_2 is higher at the highest current density for electrocoagulation with vibration-induced plates suggesting that the particle aggregation rate was higher when vibration-induced plates were applied and lower when the plates were static.

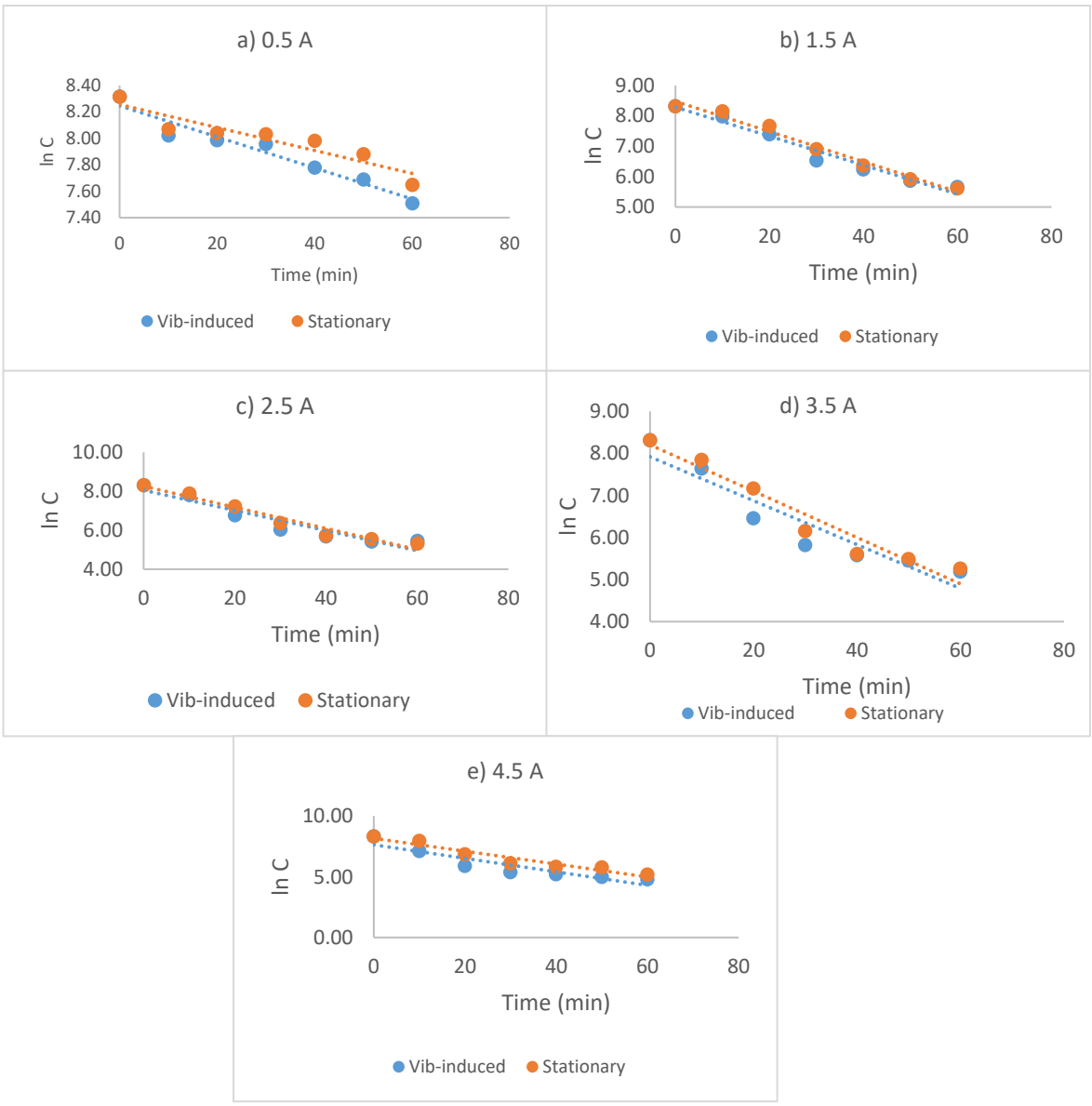

Figure 4. Plot of first-order reaction at Kinetics data at a) 0.5 A b) 1.5 A c) 2.5 A d) 3.5 A e) 4.5 A

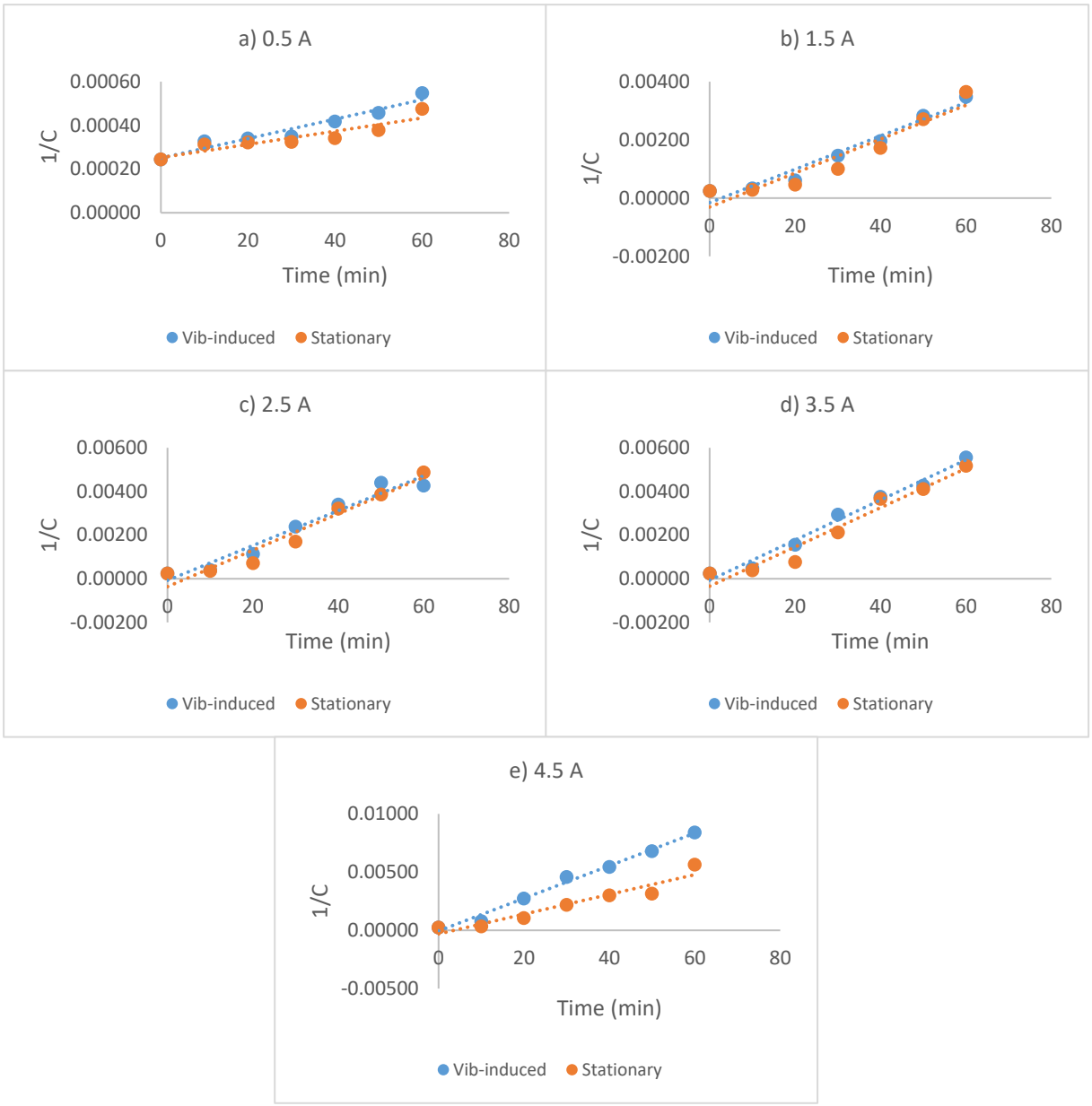

Figure 5. Plot of second-order reaction kinetics data at a) 0.5 A b) 1.5 A c) 2.5 A d) 3.5 A e) 4.5 A

Analysis of Particle Distribution Behaviour

The particle distribution behaviour was analysed regarding the concentration of colour removal using the rate constant k_2, as obtained from the previous kinetic study. The general trend of particle aggregation during electrocoagulation-flocculation is depicted in Figure 6. It is seen that there is a significant reduction of the singlet particles over a short period, referred to the rapid coagulation. During this period, particles are predominantly attracted to opposite charges until they stabilise fully, increasing the number of doublet and triplet particles. Once stabilised, the particles aggregating in this region comprise flocculation; hence, a more extended period is observed.

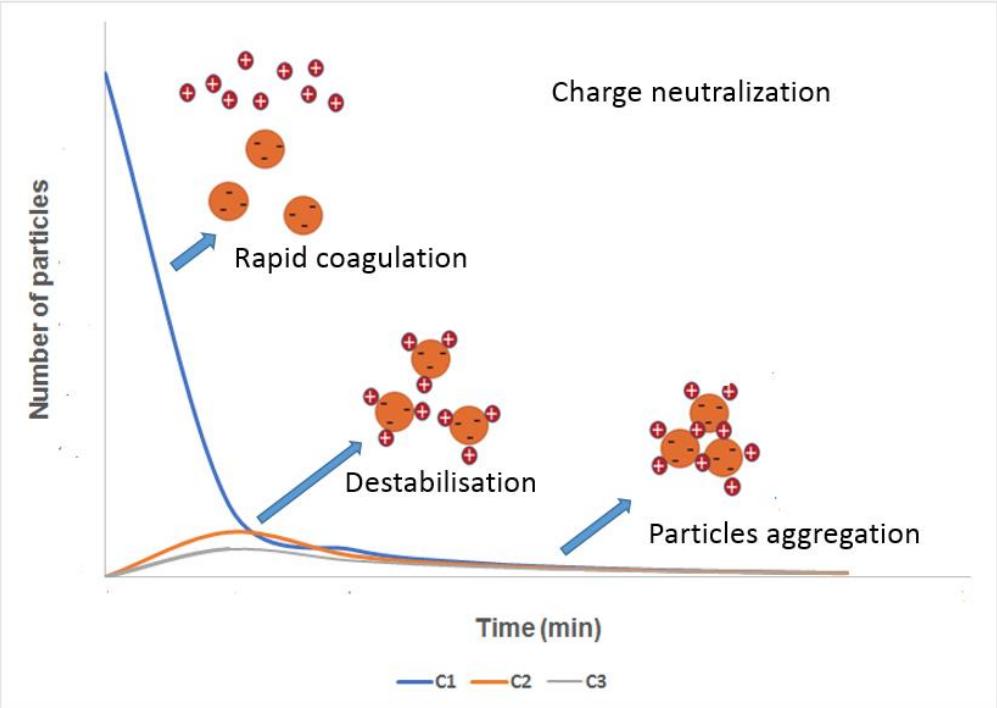

Figure 6. Particles aggregation as a function of the number of particles and time

Figures 7 and 8 show the results of the particle distribution of C_1, C_2 and C_3 for electrocoagulation with vibration-induced and stationary plates, respectively. Considering that the rate constant k_2 in electrocoagulation with vibration-induced plates is higher than that for stationary plates, the number of particles observed over time is lower in electrocoagulation with vibration-induced plates. Nevertheless, both figures showed similar trend concerning the time evolution of particles. The number of mono particles (C_1) decreased more rapidly as the doublets (C_2) and triplets (C_3) increased. It was attributed to the formation of doublets and triplets for rapid destabilisation of monomers, facilitating coagulation. These observations align with Ugonabo et al. (2016) and Igwegbe et al. (2021). According to Menkiti et al. (2011), this distribution profile can be associated with moderately rapid destabilisation of charged particles which was depicted by the moderately hyper slope with time. It can also be shown that Brownian coagulation is dominant for primary (or tiny) particles (Ugonabo et al., 2012). Therefore, electrocoagulation with vibration-induced plates produced gas bubbles and particles with Brownian movement following the induced flow, with charge neutralisation being depicted as the dominant coagulation-flocculation mechanism in this distribution.

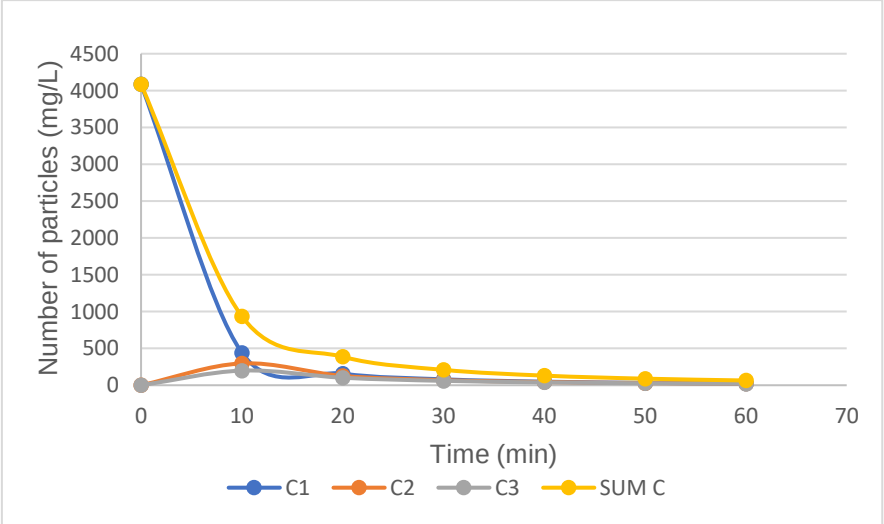

Figure 7. Particle distribution in electrocoagulation with vibration-induced plates

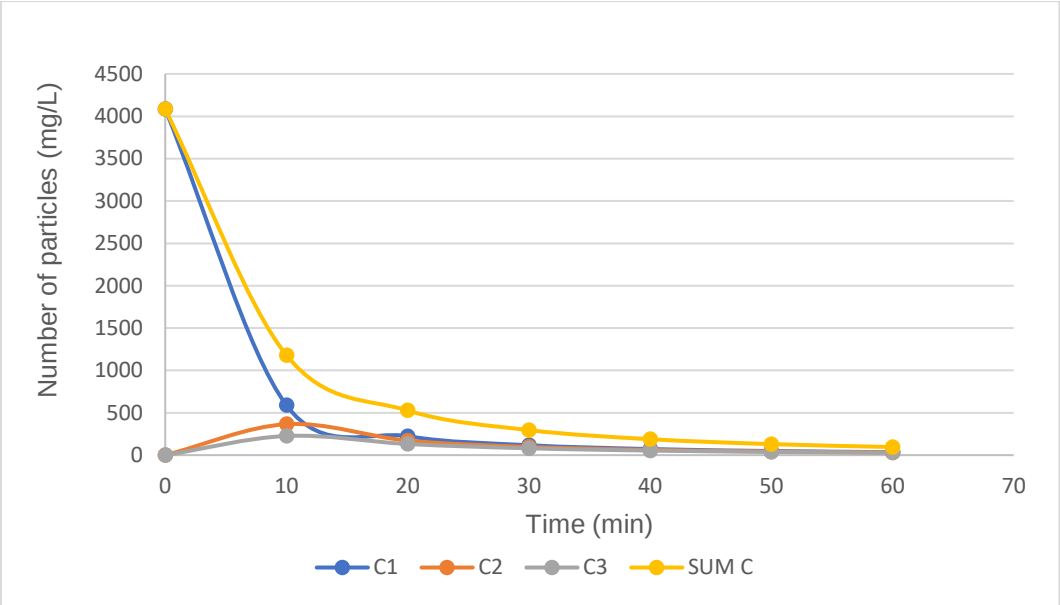

Figure 8. Particle distribution in electrocoagulation with stationary plates

CONCLUSION

This study assessed the performance of electrocoagulation with vibration-induced plates in terms of the assessment on the plate resistance, colloidal stability, coagulation-flocculation kinetics and particle distribution behaviour. In the study on the effect of resistance on electrocoagulation, it can be concluded that the plate resistance, R_p that occurred on the electrode surface was due to the accumulation of gas bubbles surrounding the plate. Without any enforced agitation as in electrocoagulation with stationary plates, the accumulation and adherence of gas bubbles is dominant, preventing effective ions transport between plates. At constant vibration intensity of 2.8 V and at initial pH of 5, the electrocoagulation using vibration-induced plates was able to lower 4% - 20% of the overall resistance as compared to electrocoagulation with stationary plates.

Analysis on the zeta potential found that the vibration-induced electrocoagulation achieved coagulation-flocculation in a faster rate within 20 – 30 minutes of time as compared to electrocoagulation with stationary plates which was achieved within 50 minutes of time. The kinetics of electrocoagulation with vibration-induced plate showed that the data fit with the second-order reaction model with the highest R^2 value of 0.9890 and the rate constants of 0.0001 $L.mg^{-1}min^{-1}$. This rate constant is higher than that achieved by electrocoagulation using stationary plates, which is 8 x 10^{-5} $L.mg^{-1}min^{-1}$ of the same reaction order and can be described to fit the theory of Brownian diffusion proposed by Von Smoluchowski (1917). The particle distribution profile showed that the number of particles reduced over time and was associated with the rapid destabilisation of charged particles. It is further concluded that the induced flow created by plate vibration enhanced the flotation rate, suggesting that charge neutralisation was the dominant electrocoagulation mechanism.

For future studies, other than using stationary plates, another comparison study can be expanded which vary the agitation mechanism in electrocoagulation such as using the magnetic stirring or other type of mechanical stirring in the electrocoagulation cell. Performance can be distinguished with the vibration-induced plates in terms of the determination of overall resistance, removal efficiency as well as gas characteristics and flow behaviour using these agitators.

ACKNOWLEDGEMENTS

The research is funded by the Ministry of Higher Education Malaysia through the Fundamental Research Grant Scheme (FRGS) (ref: FRGS/1/2019/TK10/USM/03/1).

REFERENCES

1. Kamaruddin, M. A., Abdullah, M. M. A., Yusoff, M. S., Alrozi, R. & Neculai, O. (2017) Coagulation-Flocculation Process in Landfill Leachate Treatment: Focus on Coagulants and Coagulants Aid. *IOP Conference Series of Material Science and Engineering*, **209**.

2. Moussa, D. T., El-Naas, M. H., Nasser, M. & Al-Marri, M. J. (2017) A comprehensive review of electrocoagulation for water treatment: Potentials and challenges. *J. Environmental Management*, **186**, 24–41.

3. Sitorus, I. S., Astono, W. & Iswanto, B. (2018) Batch leachate treatment using stirred electro-coagulation reactor with variation of residence time and stirring rate Batch leachate treatment

using stirred electrocoagulation reactor with variation of residence time and stirring rate. *IOP Conference Series ofvEarth and Environmental Science*, **106**.

4. Gilpavas, E., Dobrosz-Gómez, I. & Gómez-García, M. Á. (2019) Optimization and toxicity assessment of a combined electrocoagulation, H2O2/Fe2+/ UV and activated carbon adsorption for textile wastewater treatment. *Science of the Total Environment*, **651**, 551–560.

5. Al-Raad, A. A. *et al.* (2019) Treatment of saline water using electrocoagulation with combined electrical connection of electrodes. *Processes*, **7**.

6. Huang, H., Zhang, D., Zhao, Z., Zhang, P. & Gao, F. (2017) Comparison investigation on phosphate recovery from sludge anaerobic supernatant using the electrocoagulation process and chemical precipitation. *Journal of Clean Production*, **141**, 429–438.

7. Al-Raad, A. A., Hanafiah, M. M., Naje, A. S. & Ajeel, M. A. (2020) Optimized parameters of the electrocoagulation process using a novel reactor with rotating anode for saline water treatment. *Environmental Pollution*, **265**.

8. Zhu, L. *et al.* (2011) An on-demand microfluidic hydrogen generator with self-regulated gas generation and self-circulated reactant exchange with a rechargeable reservoir. *Microfluidics and Nanofluidics*, **11**, 569–578.

9. Angulo, A., van der Linde, P., Gardeniers, H., Modestino, M. & Fernández Rivas, D. (2020) Influence of Bubbles on the Energy Conversion Efficiency of Electrochemical Reactors. *Joule*, **4**, 555–579.

10. Peñas, P. *et al.* (2019) Decoupling Gas Evolution from Water-Splitting Electrodes. *Journal of The Electrochemical Society*, **166**, H769–H776.

11. Groß, T. F., Bauer, J., Ludwig, G., Fernandez Rivas, D. & Pelz, P. F. (2018) Bubble nucleation from micro-crevices in a shear flow: Experimental determination of nucleation rates and surface nuclei growth. *Experiments in Fluids*, **59**.

12. Hadikhani, P. *et al.* (2018) Inertial manipulation of bubbles in rectangular microfluidic channels. *Lab on a Chip*, **18**, 1035–1046.

13. Muhammad Niza, N.,Yusoff, M. S., Mohd Zainuri, M. A. A., Emmanuel, M. I., Mohamed Hussen Shadi, A. B., Kamaruddin, M. A. (2020) Performance of batch electrocoagulation with vibration-induced electrode plates for landfill leachate treatment. *Journal of Water Process Engineering*, **36**, 101282.

14. Muhammad Niza, N., Yusoff, M. S., Mohd Zainuri, M. A. A., Emmanuel, M. I., Mohamed Hussen Shadi, A. B., Mohd Hanif, M. H., Kamaruddin, M. A. (2021) Removal of Ammoniacal Nitrogen from Old Leachate using Batch Electrocoagulation with Vibration-induced Electrode Plate. *Journal of Environmental Chemical Engineering*, **9**, 105064.

15. Muhammad Niza, N., Abdul Razak, N., Yusoff, M. S., Mohd Zainuri, M. A. A., Emmanuel, M. I., Mohamed Hussen Shadi, A. B., Mohd Hanif, M. H., Kamaruddin, M. A. (2020) Hydrodynamic study of bubble characteristics and bubble rise velocities in batch electrocoagulation with vibration-induced electrode plates using the PIV technique. *Separation and Purification Technology*, **258**, 118089.

16. Baird, R., Rice, E. W., Eaton, A. D., Bridgewater, L. & Federation, W. E. (2017) *Standard Methods for the Examination of Water and Wastewater* (American Public Health Association).

17. Al-Qodah, Z. & Al-Shannag, M. (2017) Heavy metal ions removal from wastewater using electrocoagulation processes: A comprehensive review. *Separation Science and Technology*, **52**, 1–28.

18. Wang, K. L., Yung-Tse, H. & K.Shammas, N. (2005) *Ozonation*. *Handbook of Environmental Engineering, Volume 3: Physicochemical Treatment Processes*. Humana Press, doi:10.1385/1-59259-820-x:315.

19. Shammas, N. K. (2005) Coagulation and Flocculation - Physicochemical Treatment Processes. in (eds. Wang, L. K., Hung, Y.-T. & Shammas, N. K.) 103–139. Humana Press. doi: 10.1385/1-59259-820-x:103.

20. Ghernaout, D. (2015) Brownian Motion and Coagulation Process. *American Journal of Environmental Protection*, **4**, 1.

21. Ghernaout, D., Naceur, M. W. & Ghernaout, B. (2011) A review of electrocoagulation as a promising coagulation process for improved organic and inorganic matters removal by electrophoresis and electroflotation. *Desalination of Water Treatment*, **28**, 287–320.

22. Smoluchowski, V. M. (1917) Versuchcheiner mathematischen theorie der koagulations koagulations kinetic kolloider lousungen. *Physical Chemistry*, 129–168.

23. Menkiti, M. C., Onyechi C. A. & Onukwuli, O. D. (2011) Evaluation of Perikinetics Compliance for the coagflocculation of Brewery Effluent by Brachystegia eurycoma Seed Extract. *International Journal of Multidisciplinary Sciences and Engineering*, **2**, 73–80.

24. Menkiti, M. C., Igbokwe, P. K., Ugodulunwa, F. X. O. & Onukwuli, O. D. (2008) Rapid Coagulation/Flocculation Kinetics of Coal Effluent with High Organic Content Using Blended an dUNblended Chitin Derived Coagulant (CSC). *Research Journal of Applied Sciences*, **3**, 317–323.

25. Menkiti, M. C. & Ejimofor, M. I. (2016) Experimental and artificial neural network application on the optimization of paint effluent (PE) coagulation using novel Achatinoidea shell extract (ASE). *Journal of. Water Process Engineering*, **10**, 172–187.

26. Ugonabo, V. I., Emembolu, L. N. & Igwegbe, C. A. (2016) Bio-Coag-Flocculation of Refined Petroleum Wastewater using Plant Extract: A Turbidimeric Approach. *International Journal of Emerging Engineering Research and Technology*, **4**, 19–26.

27. Ugonabo, V., Menkiti, M. C. & Onukwuli, O. (2012) Coagulation Kinetics and Performance Evaluation of Corchorus Olitorus Seed in Pharmaceutical Effluent.

28. Naje, A. S., Chelliapan, S., Zakaria, Z., Ajeel, M. A. & Adeniyi Alaba, P. (2016) A review of electrocoagulation technology for the treatment of textile wastewater. *Reviews in Chemical Engineering*, **33**, 1–30.

29. Huijuan, L., Xu, Z. & Jiuhui, Q. (2010) Electro-coagulation in water treatment. *Electrochemistry for the Environment*, 252–269.

30. Mohtashami, S. R. (2018) Electroflotation for Treatment of Paint Wastewater : Experiments, Kinetics and Hydrodynamics.

31. Igwegbe, C. A., Onukwuli, O. D., Ighalo, J. O. & Umembamalu, C. J. (2021) Electrocoagulation-flocculation of aquaculture effluent using hybrid iron and aluminium electrodes: A comparative study. *Chemical. Engineering Journal Advances*, **6**, 100107.